

Classification of built-up areas in LiDAR data based on second-generation connectivity filters

Robi Cvirn*

Supervised by: Domen Mongus[†]

University of Maribor / Slovenia

Abstract

In the recent years, Light Detection and Ranging (LiDAR) technology has become one of the prime technologies for spatial data acquisition. By rapid and accurate capturing of high-resolution 3D point-clouds, LiDAR has moved the focus of further research in Earth Observations towards data processing. In this paper, we propose a new approach for classification of built-up areas from LiDAR data. The methodology is based on a special class of morphological filters that rely on so-called second-generation connectivity. We first provide theoretical background on connected operators and explain how they can be applied for LiDAR data processing. Finally, we validate the proposed approach on several testcases.

Keywords: LiDAR, mathematical morphology, second-generation connectivity, object recognition, algorithms

1 Introduction

Light Detection and Ranging (LiDAR) technology has become one of the prime technologies for acquiring high-resolution spatial data. By rapidly capturing accurate 3D point-clouds of the Earth's surface, it allows for monitoring structures and processes with great precision over vast geographic areas. Over the past decade, a lot of research has been directed towards object recognition in LiDAR data and efficient methods for extracting ground [9, 10], buildings [8, 13, 20], vegetation [5], and even single tree-crowns [4, 11] have already been developed. The focus of further research is now shifting towards situation assessment, where recognized objects are taken into account in order to establish a wider sense of the current situation. A particularly important example of situation assessment is a classification of built-up areas, as it is critical for many studies of impacts that human developments have on the natural process [7].

In this paper, a new method for the classification of built-up areas is presented. In contrast to the related work, the proposed method has a different approach by exploiting the height information present within the LiDAR

data. This is achieved by connected operators from the framework of mathematical morphology that are based on second-generation connectivity.

The related work is described in Section 2. The relevant theoretical background is given in Section 3. Section 4 describes the data structuring needed in order to apply connected operators for LiDAR data processing together with the proposed method. The results are discussed in Section 5. Section 6 concludes the paper.

2 Related work

The classification of built-up areas has up to now been mostly achieved based on human intuition by considering the actual size of the area (and its population) in addition to the services that a given area offers (e.g. by the presence of education and medical institutions, train stops, or sports buildings) [1]. Nevertheless, several approaches have already been developed that rely on satellite images for delivering quantitative measurement of built-up areas for their classification. Pesaresi et. al [17] proposed a method for calculating built-up presence index from panchromatic satellite images. Tomowski et. al [25] developed a settlement area detection based on panchromatic and multispectral data, while Najab et. al [12] introduced a classification of settlements based on holistic feature extraction technique using high resolution satellite images. Van den Bergh [26] proposed a method for classification of settlements based in their illumination geometry in QuickBird images.

3 Theoretical background

This section describes theoretical basics of connected operators within the context of mathematical morphology. Let a universal nonempty set $E \subseteq \mathbb{R}^d$ (i.e. a definition domain), define a d -dimensional dataset (e.g. a binary 2D image, 3D voxel space, or any higher dimensional discrete set) is defined by the means of nonempty set $S \subseteq E$, where $s_i \in S$ is a d -dimensional point. A power-set (i.e. a set of all subsets of set S) is denoted as $\mathcal{P}(S)$, while the connectivity between the elements of S is given by the means of

*robi.cvirn@um.si

[†]domen.mongus@um.si

connectivity class $\mathcal{C} \subseteq \mathcal{P}(S)$ [15, 22, 23, 24]. For this purpose, \mathcal{C} has to satisfy the following two conditions[16]:

- $\emptyset \in \mathcal{C}$ and $\forall s_i \in S, s \in \mathcal{C}$ and
- $\forall \{C_i\} \subseteq \mathcal{C}, \cap_i C_i \neq \emptyset \Rightarrow \cup_i C_i \in \mathcal{C}$.

In simple terms, this means that an empty set, any given singleton, and any set of subsets $C_i \subseteq S$ with non-empty intersection is connected. Given $s_i \in S$, the corresponding connected component of a set S can be extracted by the connectivity opening Γ . Its formal definition is given as [16]:

$$\Gamma_{s_i}(S) = \bigcup_j \{C_j \in \mathcal{C} \mid s_i \in C_j \text{ and } C_j \subseteq S\}. \quad (1)$$

In order to simplify the notation, we refer to the connected component addressed by a point s_i as $C_i = \Gamma_{s_i}(S)$.

3.1 Connected operators

Connected operators within the framework of mathematical morphology are edge preserving operators that act directly on connected components [21]. Attribute filters are well-known examples of connected operators. They allow for filtering connected components according to their attributes. Let attribute function of a connected component Λ (e.g. its area, perimeter or width) and the corresponding attribute threshold λ , a binary attribute opening of an arbitrary set S is given as [14]:

$$\Gamma_{(\Lambda, \lambda)}(S) = \bigcup_{s_i \in S} \{\Gamma_{(\Lambda, \lambda)}(\Gamma_{s_i}(S))\}, \quad (2)$$

where attribute opening $\Gamma_{(\Lambda, \lambda)}(S)$ removes those connected components of S that do not satisfy a given attribute criteria $\Lambda(C_i) \geq \lambda$ (i.e. $\Gamma_{(\Lambda, \lambda)}(S) = \{C_i \mid \Lambda(C_i) \geq \lambda\}$).

3.2 Second-generation connectivity

Each connectivity class \mathcal{C} can be evolved to its child class with curtailed or augmented members. This concept is known as second-generation connectivity and it allows for manipulation over the connected components that can not be achieved by regular connected operators. Two types of second-generation connectivity exist, namely contraction-based connectivity that allows for braking the connected components and clustering-based connectivity that allows for merging them [3]. Due to the specifics of the proposed method, (see Section 4), only the latter is considered in this paper.

A cluster can be described as a set of connected components for which the mutual distances between them are smaller than a certain distance criteria. In order to achieve clustering, a clustering operator ψ needs to be applied that complies to the following restrictions [19, 23, 3]:

- ψ needs to be extensive and increasing,

- the resulting connectivity class has to be reduced or equal to the input connectivity class $\psi(\mathcal{C}) \subseteq \mathcal{C}$, and
- for all subsets of a set $\{S_i\} \in \mathcal{P}(S)$ it is required that $\forall i, \psi(S_i) \in \mathcal{C}$, and $\cap_i S_i \neq \emptyset \Rightarrow \psi(\cup_i S_i) \in \mathcal{C}$.

Let ψ be a clustering operator on $\mathcal{P}(S)$ and \mathcal{C} a connectivity class in $\mathcal{P}(S)$, a clustering-based connectivity class $\mathcal{C}^\psi \supseteq \mathcal{C}$ within the definition domain E can than be defined as:

$$\mathcal{C}^\psi = \{S \in \mathcal{P}(E) \mid \psi(S) \in \mathcal{C}\}. \quad (3)$$

By only redefining the elementary connectivity opening, this allows for applying second-generation connectivity together with any of the connected operators without changing their original definitions. A second-generation connectivity opening $\Gamma_{(\Lambda, \lambda)}^\psi(S)$, defined in regards to an arbitrary attribute function Λ with attribute threshold λ is given as [15]:

$$\Gamma_{(\Lambda, \lambda)}^\psi(S) = \Gamma_{(\Lambda, \lambda)}(\psi(S)) \cap S. \quad (4)$$

Finally, the results of the second-generation connectivity opening $\Gamma_{(\Lambda, \lambda)}^\psi(S)$ applied on a binary image S are shown in Fig. 1.

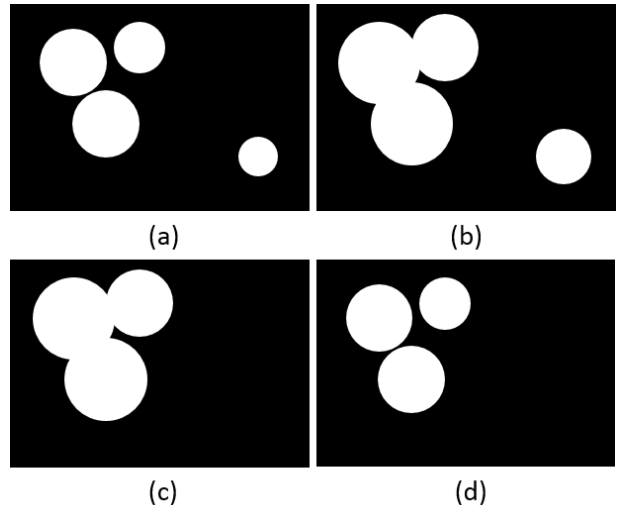


Figure 1: Second generation attribute opening, where (a) the original image S is (b) extended by a clustering operator $\psi(S)$ and (c) attribute opening is applied $\Gamma_{(\Lambda, \lambda)}(\psi(S))$ in order to obtain (d) the resulting set $\Gamma_{(\Lambda, \lambda)}^\psi(S)$.

4 Implementation of connected operators on LiDAR data

We denote an input LiDAR point-cloud as $P = \{P_i\}$ where p_i is an individual LiDAR point. Each p_i is associated with a coordinate triple, given as $x(p_i)$, $y(p_i)$, and $z(p_i)$. Note

that connected operators, as described in previous section, can not be directly applied on P , due to the lack of its topological structure. In order to overcome this issue, we construct a grid $G \subset \mathbb{R}^2$ of resolution r (usually $r = 0.5m$ is sufficient) and the extent that is equal to the bounding-box of P . A grid-cell is denoted as $g_i \in G$, while a set of LiDAR points that are closer to a given g_i than to any other $g_j \in G$ are denoted as $P_{g_i} \subseteq P$. In continuation, we demonstrate the efficiency of the proposed formulation for the classification of built-up areas.

4.1 Classification of built-up areas

The main objective of this method is to classify the built-up areas according to their sizes and heights of the contained buildings. The method uses preprocessed LiDAR data, where points belonging to buildings are already classified. In our case, were detected by extracting linearly distributed points using Locally Fitted Surfaces and measuring their geometric properties based on differential morphological profiles[8]. We can thus define a function $\text{class} : P \rightarrow [\text{building}, \text{not building}]$ that returns a classification of a LiDAR point. A set of building grid-cells $S \subseteq G$ is formally defined by Eq. 5, while its meaning is graphically explained in Fig. 2.

$$S = \{g_i \in G \mid \exists p_j \in P_{g_i} \text{ and } \text{class}(p_j) = \text{building}\}. \quad (5)$$

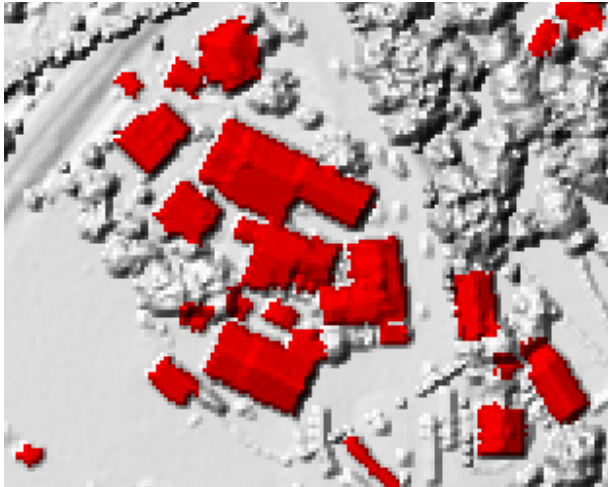


Figure 2: The definition of $S \subseteq G$, according to the buildings (colored red) contained within the input LiDAR dataset.

Each connected component represents a building and is a set of a 8-connected cells (i.e. $C_i \subset S$). In the next step, we apply a clustering-based second-generation connectivity on the set of connected components contained in S . Since spatial distance between buildings within the built-up areas may vary, spatially-variant clustering operator is an optimal choice [2]. As shown by the results (see

Section 5), sufficient accuracy is achieved by using a morphological dilation with the size of the structuring element that is directly proportional to the heights of the buildings contained within the corresponding connected components $C_i \in S$. Let $h : G \rightarrow \mathbb{R}$, be a height function, defined at a given $g_i \in G$ as:

$$h(g_i) = \bigvee_{g_j \in C_i} \{h(p_l) \mid p_l \in P_{g_j}\}, \quad (6)$$

where \bigvee denotes supremum (i.e. maximum). In addition, when $P_{g_i} = \emptyset$, $h = 0$. A clustering operator in a form of morphological dilation with variable window size is then denoted as $\delta^{t^S h}$, where t^S is a user defined parameter that defines the linear relationship between the heights of the buildings and the corresponding size of the structuring element. The results of $\delta^{t^S h}(S)$ are shown in Fig. 3.

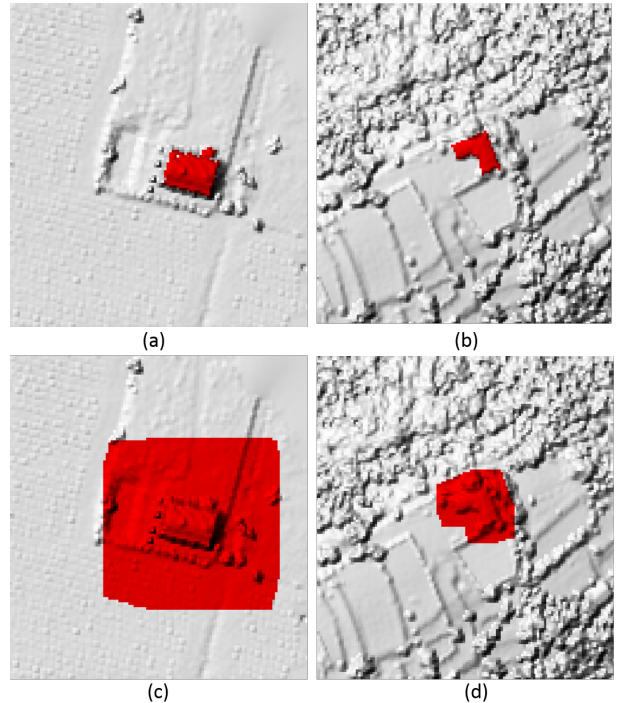


Figure 3: The spatially-variable dilation $\delta^{t^S h}$, applied on (a and b) two connected components of different heights (i.e. 13m and 6m, respectively) and (c and d) the obtained results.

According to Eq. 4, second-generation connectivity opening that removes those connected components C_i with areas $A(C_i) < a$ can now be given as $\Gamma_{(\lambda, \lambda)}^{\delta^{t^S h}}$. According to the literature, built-up areas may be divided into hamlets, villages, towns and cities [1]. In order to identify the correct type, we apply a series of second-generation connectivity openings at an increasing scale and observe those connected components (i.e. buildings) removed at each of the scales. This concepts is also known as differential attribute profiles [14]. Let $a_1 = 50000m^2$, $a_2 = 1000000m^2$,

and $a_3 = 5000000m^2$ be a set of user defined area thresholds that correspond to the areas of particular built-up types (note that this particular values were intuitively defined, as there is no actual standard definition of the terms [1]). We may define a set of buildings belonging to each of them by the following rules:

- Hamlets $S^H = S \setminus \Gamma_{(A,a_1)}^{\delta^{r^S_h}}(S)$
- Villages $S^V = \Gamma_{(A,a_1)}^{\delta^{r^S_h}}(S) \setminus \Gamma_{(A,a_2)}^{\delta^{r^S_h}}(S)$
- Towns $S^T = \Gamma_{(A,a_2)}^{\delta^{r^S_h}}(S) \setminus \Gamma_{(A,a_3)}^{\delta^{r^S_h}}(S)$, and
- Cities $S^C = \Gamma_{(A,a_3)}^{\delta^{r^S_h}}(S)$.

The obtained results are shown in Fig. 4.

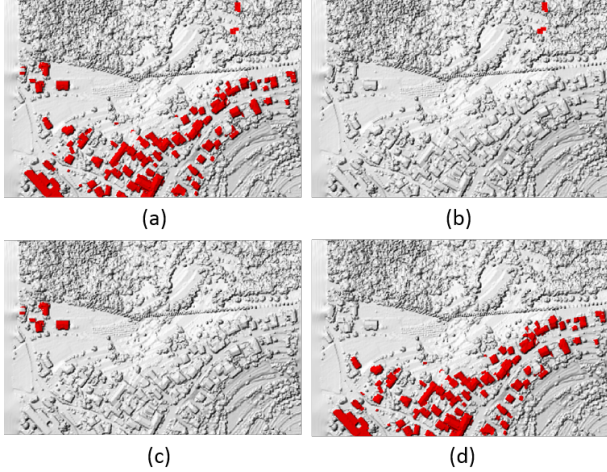


Figure 4: Differential attribute profiles on second-generation connectivity opening, where (a) the original S is divided into (b) hamlets S^H , (c) villages S^V , and (d) towns S^T .

5 Results

The proposed method for classification of built-up areas was tested on four different LiDAR datasets. Each of them contained different types of built-up areas as well as different terrain configurations and was acquired at different data densities. Details about particular test set are given in Table 1.

5.1 Validation procedure

To verify the quality of classification, the obtained results were compared with ground truth data. For this purpose, land cadastral data was rasterized and its actuality was checked by a domain expert. In this way, we were able

Table 1: Test datasets with description.

Dataset name	Description	Terrain type	Data density [points per m^2]
RA	Rural area with hamlets and villages	hilly	7.3
TS	Town and nearby small settlements	valley	8.7
CS	City and its suburb	flat	12.6
CC	Strict city center	flat	5.5

to perform a grid-cell to grid-cell comparison, where true positives (TP), false positives (FP), true negatives (TN), and false negatives (FN) were measured for each of the classes. Accordingly, the following measurements of quality were used for validation [18, 6]:

- Completeness, describing the rate of correctly recognized classes, is defined as:

$$comp = \frac{TP}{TP + FN}, \quad (7)$$

- Correctness, describing the rate of correct detection, is defined as:

$$corr = \frac{TP}{TP + FP}, \text{ and} \quad (8)$$

- F1-score that is harmonic mean of completeness and correctness is given by:

$$F1 = 2 * \frac{comp \cdot corr}{comp + corr}. \quad (9)$$

5.2 Sensitivity analysis

As explained in Section 4, the proposed method uses one input parameter t^S that defines the linear relation between the heights of the buildings and the size of the structuring element in spatially-variant dilation. In order to provide its optimal definition, we were progressively increasing the value of t^S , while measuring the success rate of the method. The obtained results are shown in Table 2.

Table 2: Sensitivity analysis of the method in regards to the parameter t^S , presented by F1-score.

Dataset	t^S				
	0.5	1.0	1.5	2.0	3.0
RA	50.5	86.3	96.7	35.9	36.3
TS	10.9	18.8	91.4	96.1	94.5
CS	17.7	33.7	43.4	93.2	54.9
CC	73.4	91.2	94.3	94.2	95.2

As shown by Table 2, the proposed method is sensitive to the value of t^S due to significantly different spacing of buildings within the different types of built-up areas. This indicates that, by defining the size of the clustering operator according to the correspondent height of the building, the issue can only be mitigated but it cannot be solved. Still, the proposed method managed to achieve accuracy of over 93% in all of the cases.

5.3 Validation

A closer look at Table 2 reveals that low t^S values are more appropriate for classifying datasets containing rural or suburb areas, while large t^S values are more suitable for classifying datasets containing city areas. The main reason for this is that hamlets do not require any clustering in order to be successfully recognized, while high buildings in city areas are often widely spaced with green areas or parking lots between them. A more detailed analysis of the method's quality and accuracy was therefore performed using optimal definition of t^S for each particular test dataset. The obtained results are shown in Table 3 and Fig. 5.

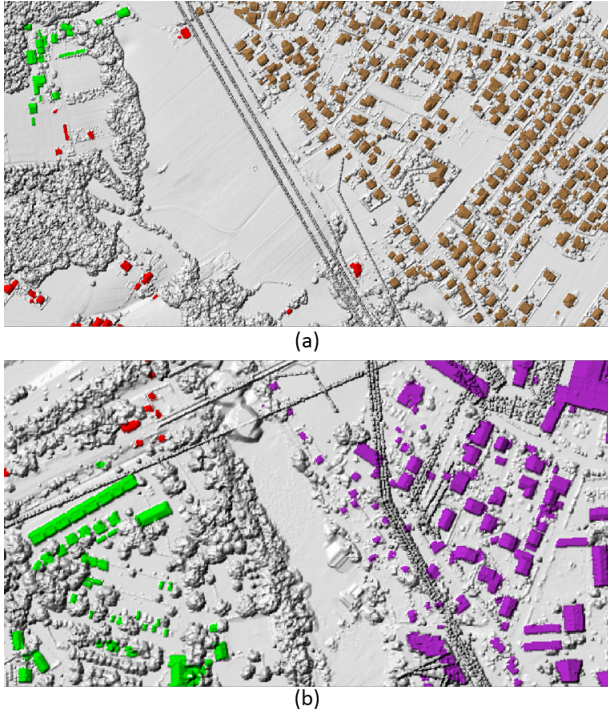


Figure 5: Examples of classified datasets containing (a) a city (colored brown), nearby village (colored green), and hamlets (colored red) and (b) a town (colored purple) with several nearby hamlets.

As shown by Table 3, the proposed method achieves average F1-score of over 87% per all classes, with average completeness as well as correctness close to 90%.

However, large deviations in the results can be noticed when considering hamlets or villages. The main reason for this is that these are relatively small types of settlements, where error in the classification of a single building significantly affects the overall accuracy. Nevertheless, most of the inaccuracies are caused by two characteristic errors. Namely, isolated low buildings within towns (see an example in Fig. 6) and groups of hamlets containing relative tall buildings that become clustered and recognized as a town or a village (see example in Fig. 7). Still as shown in Table 4, the classification of the built-up areas is significantly more efficient than the traditional approach, where building heights are not considered in a clustering criterion. In latter case, the used clustering criterion was based on the area attribute of the regions, while the same tuning procedure as described in Section 5.2 was used. Although the proposed approach achieves higher accuracy, the compared method can also be applied on other types of data, where object heights are not explicitly known (e.g. satellite images [17, 12] or digital orthophoto [26]).

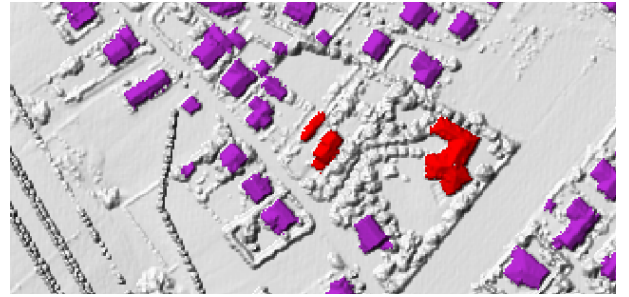


Figure 6: Missclassified low buildings (colored red) within a town (colored purple).

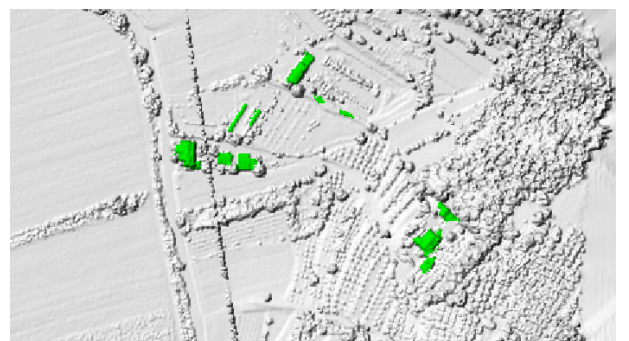


Figure 7: Missclassified hamlets, clustered into a village due to the contained high buildings.

6 Conclusions

This paper proposes a new method for the classification of built-up areas in LiDAR data. The method is based on

Table 3: Validation results of built-up area classification.

Dataset	t^S	Metric	Built-up area types			
			S^H	S^V	S^T	S^C
RA	1.5	comp	100	96.1	not contained	not contained
		corr	82.5	100	not contained	not contained
		F1	90.4	98.0	not contained	not contained
TS	2.0	comp	64.5	97.9	100	not contained
		corr	95.2	88.7	95.0	not contained
		F1	76.9	93.1	97.5	not contained
CS	2.0	comp	96.5	77.8	not contained	98.9
		corr	86.2	87.5	not contained	100
		F1	91.1	82.4	not contained	99.4
CC	3.0	comp	not contained	100	not contained	96.9
		corr	not contained	0	not contained	100
		F1	not contained	0	not contained	98.4
Average	-	comp	87.0	93.0	100	97.9
		corr	88.0	69.1	95.0	100
		F1	86.1	68.4	97.5	98.9

Table 4: Analysis of the method with clustering criterion based on the area attribute of the regions, presented by F1-score.

Dataset	t^S				
	0.01	0.03	0.05	0.10	1.00
RA	26.9	78.8	93.4	32.5	0.0
TS	17.7	86.9	76.6	58.9	0.0
CS	11.0	93.0	92.4	91.8	85.6
CC	87.8	91.6	93.0	94.1	92.0

mathematical morphology, where connected operators of second-generation are used for clustering buildings into groups of built-up areas. As the method uses only one user defined parameter, its performance can simply be optimized, although the method is relatively sensitive to it. Nevertheless, with the average F1-score of 93%, the proposed method proved to be accurate.

References

- [1] M. Aston. *Interpreting the landscape*. B.T.Batsford Ltd, 1985.
- [2] N. Bouaynaya, M. Charif-Chetchaouni, and D. Schonfeld. Theoretical foundations of spatially-variant mathematical morphology part i: Binary images. *Pattern Analysis and Machine Intelligence, IEEE Transactions on*, 30(5):823–836, May 2008.
- [3] U. Braga-Neto and J. Goutsias. Connectivity on complete lattices: New results. *Computer Vision and Image Understanding*, 85:22–53, 2002.
- [4] L. Eysn, M. Hollaus, E. Lindberg, F. Berger, J. M. Monnet, M. Dalponte, M. Kobal, M. Pellegrini, E. Lingua, D. Mongus, and N. Pfeifer. A benchmark of lidar-based single tree detection methods using heterogeneous forest data from the alpine space. *Forests*, 6(5):1721–1747, May 2015.
- [5] S. Hancocka, J. Armston, Z. Li, R. Gaulton, P. Lewis, M. Disney, F. M. Danson, A. Strahler, C. Schaaf, K. Anderson, and K. J. Gaston. Waveform lidar over vegetation: An evaluation of inversion methods for estimating return energy. *Remote Sensing of Environment*, 164:208–224, July 2015.
- [6] C. Heipke, H. Mayer, and C. Wiedemann. Evaluation of automatic road extraction. *3d Reconstruction and Modeling of Topographic Objects*, 32:151–160, September 1997.
- [7] A. Mabogunje. *The development process: A spatial perspective*. Routledge, 2015.
- [8] D. Mongus, N. Lukac, and B. Zalik. Ground and building extraction from lidar data based on differential morphological profiles and locally fitted surfaces. *ISPRS Journal of Photogrammetry and Remote Sensing*, 93:145–156, July 2014.
- [9] D. Mongus and B. Zalik. Parameter-free ground filtering of lidar data for automatic dtm generation. *ISPRS Journal of Photogrammetry and Remote Sensing*, 67:1–12, January 2012.
- [10] D. Mongus and B. Zalik. Computationally efficient method for the generation of a digital terrain model from airborne lidar data using connected operators. *Selected Topics in Applied Earth Observations*

- and Remote Sensing, IEEE Journal of*, 7(1):340–351, January 2014.
- [11] D. Mongus and B. Zalik. An efficient approach to 3d single tree-crown delineation in lidar data. *ISPRS Journal of Photogrammetry and Remote Sensing*, 108:219–233, October 2015.
 - [12] A. Najab, I. Khan, M. Arshad, and F. Ahmad. Classification of settlements in satellite images using holistic feature extraction. In *12th International Conference on Computer Modelling and Simulation*, 2010.
 - [13] J. Niemeyer, F. Rottensteiner, and U. Soergel. Contextual classification of lidar data and building object detection in urban areas. *ISPRS Journal of Photogrammetry and Remote Sensing*, 87:152–165, December 2014.
 - [14] G. K. Ouzounis, M. Pesaresi, and P. Soille. Differential area profiles: Decomposition properties and efficient computation. *IEEE Transactions on pattern analysis and machine intelligence*, 34(8):1533–1548, August 2012.
 - [15] G. K. Ouzounis and M.H.F. Wilkinson. Mask-based second-generation connectivity and attribute filters. *IEEE Transactions on pattern analysis and machine intelligence*, 29(6):990 – 1004, June 2007.
 - [16] G. K. Ouzounis and M.H.F. Wilkinson. Hyperconnected attribute filters based on k-flat zones. *IEEE Transactions on Pattern Analysis and Machine Intelligence*, 33(2):224–239, February 2011.
 - [17] M. Pesaresi, A. Gerhardinger, and F. Kayitakire. A robust built-up area presence index by anisotropic rotation-invariant textural measure. *IEEE Journal of selected topics in applied earth observations and remote sensing*, 1(3):180–192, September 2008.
 - [18] D. M. W. Powers. Evaluation: From precision, recall and f-factor to roc, informedness, markedness & correlation. Technical report, School of Informatics and Engineering, Flinders University, Adelaide, Australia, December 2007.
 - [19] C. Ronse. Set-theoretical algebraic approaches to connectivity in continuous or digital spaces. *Journal of Mathematical Imaging and Vision*, 8:41–58, 1998.
 - [20] F. Rottensteiner. Automation of object extraction from lidar in urban areas. In *Geoscience and Remote Sensing Symposium, 2010 IEEE International*, pages 1343 – 1346. IEEE, July 2010.
 - [21] P. Salembier and M.H.F. Wilkinson. Connected operators. *IEEE Signal processing magazine*, 26(6):136–157, November 2009.
 - [22] J. Serra. *Image Analysis and Mathematical Morphology. 2: Theoretical Advances*. Academic Press, 1988.
 - [23] J. Serra. Connectivity on complete lattices. *Journal of Mathematical Imaging and Vision*, 9:231–251, 1998.
 - [24] J. Serra. Connections for sets and functions. *Fundamenta Informaticae*, 41:147–186, 2000.
 - [25] D. Tomowski, M. Ehlers, U. Michel, and G. Bohmann. Decision based data fusion techniques for settlement area detection from multisensor remote sensing. In *1st EARSeL Workshop of the SIG Urban Remote Sensing Humboldt-Universitt zu Berlin*, 2006.
 - [26] F. van den Bergh. The effects of viewing- and illumination geometry on settlement type classification of quickbird images. In *Geoscience and Remote Sensing Symposium (IGARSS), 2011 IEEE International*, pages 1425 – 1428, July 2011.